ELECTRONIC SUPPLEMENTARY INFORMATION

Cost-effective, High-Performance Ni_3Sn_4 Electrocatalysts for Methanol Oxidation Reaction in Acidic Environments

Danil W. Boukhvalov, Gianluca D'Olimpio, Junzhe Liu, Corneliu Ghica, Marian Cosmin Istrate, Chia-Nung Kuo, Grazia Giuseppina Politano, Chin Shan Lue, Piero Torelli, Lixue Zhang, Antonio Politano

S1. Single-Crystal Growth: Single crystals of Ni_3Sn_4 were produced by the solution-growth method. Nickel powder (99.95%) and Sn ingots (99.99%) were mixed in the atomic ratio Ni:Sn = 1:20 and sealed in evacuated silica tubes. The sealed tube was heated to 750 °C at a rate of 100 °C/h, held at this temperature for 20 h, and then slowly cooled to 550 °C at a rate of 1 °C/h. Excess Sn flux was separated from the crystals using a centrifuge and diluted HCl. The obtained single crystals had a rod-like shape along the b-axis with typical dimensions of 1.5x2x5 mm^3. We first collected powder X-ray diffraction data using a Bruker D2 Phaser diffractometer. Following this, we determined the lattice parameters through Rietveld refinement with the help of the FULLPROF software package. Once the powder XRD analysis confirmed the sample as a pure phase without impurities, we proceeded to measure the XRD and Laue diffraction along the natural growth faces of single crystals.

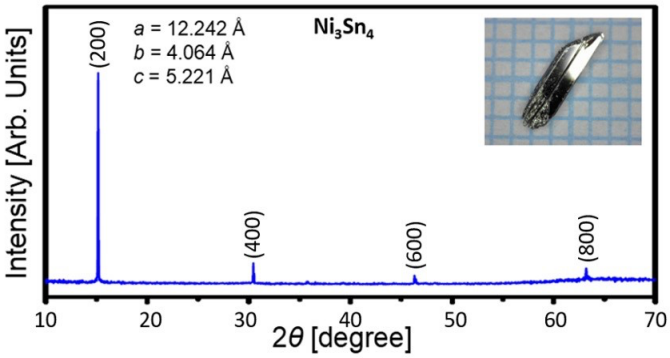

Figure S1. *XRD pattern of a Ni_3Sn_4 single crystal. The photo of grown crystals is shown in the inset.*

S2. Electrochemical measurements:

All of the electrochemical tests were conducted with a house-made three-electrode system on Biologic VSP-300 electrochemical workstation at room temperature in 0.5 M H_2SO_4 or 0.5 M H_2SO_4 + 1 M CH_3OH. Hg/Hg_2SO_4, graphite rod, and the prepared catalysts were used as the reference, counter, and working electrodes, respectively.

The linear sweep voltammetry (LSV) patterns were collected at a scan rate of 2 mV s^{-1} and the LSV curves were corrected by iR compensation with the percentage of 85. The Cyclic voltammetry (CV) patterns were collected at a scan rate of 50 mV s^{-1}. Electrochemical impedance spectroscopy (EIS) measurements were tested under 0 V vs. Hg/Hg_2SO_4 in the frequency range from 1 MHz to 100 mHz with the amplitude of 5 mV. The chronoamperometry data was collected at 0.24 V vs. Hg/Hg_2SO_4 in 0.5 M H_2SO_4 + 1 M CH_3OH solution with the scan rate of 50 mV s^{-1}.

Electric double layer capacitance (C_{dl}) of Ni_3Sn_4 was measured by cyclic voltammetry (CV) in the range of -0.02 V to 0.08 V vs. Hg/Hg_2SO_4 at the scan rates of 20, 40, 60, 80, and 100 mV s^{-1}, respectively. Electrochemical surface area (ECSA) was calculated by following equation:

$$ECSA = C_{dl}/C_s$$

where C_s was used as 35 μF cm^{-2}. To calculate the ECSA of the 20% Pt/C sample, 2 mg Pt/C was dispersed into 1 mL ink consist of 490 μL deionized water, 490 μL ethanol and 20 μL Nafion. 10 μL of the ink was coated on a graphite carbon electrode with a diameter of 3 mm. We then performed CV tests at 50 mV s^{-1} scan rate in the voltage range of -0.7 V to 0.9 V vs. Hg/Hg_2SO_4 in 0.5 M H_2SO_4. The C_{dl} of Pt/C sample is calculated by integrating CV curve and ECSA is further obtained. The durability tests were carried out at 0.24 V vs. Hg/Hg_2SO_4 in 0.5 M H_2SO_4 + 1 M CH_3OH using the Chronoamperometry technique.

The CO stripping test involved continuously flowing CO gas into 0.5 M H_2SO_4 for 30 minutes followed by continuous N_2 gas flow for another 30 minutes to remove any dissolved CO. The

adsorbed CO on the electrode was oxidized by CV at a sweep rate of 50 mVs^{-1} to obtain the CO stripping curve. Two consecutive CV curves were recorded to ensure complete oxidation of the adsorbed CO gas.

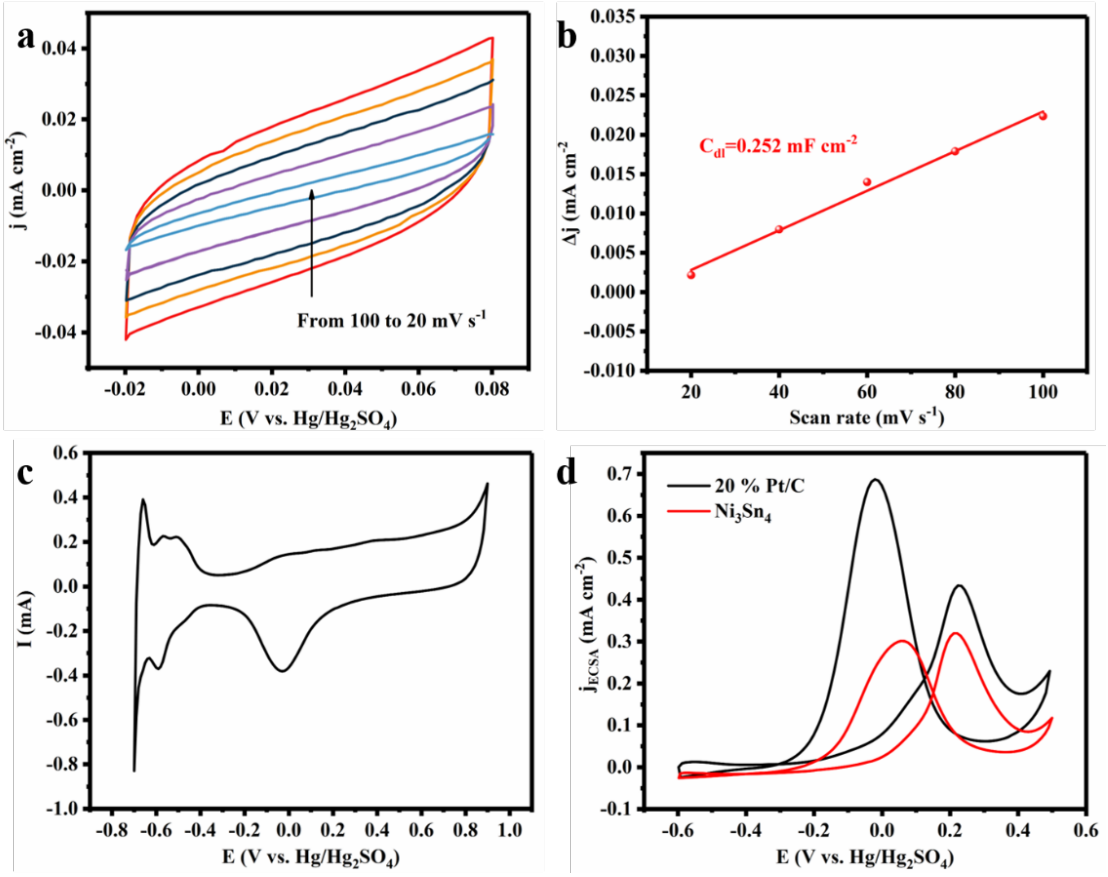

Figure S2. *(a) CV curves of Ni_3Sn_4 at the scan rates of 100, 80, 60, 40 and 20 mV/s. (b) C_{dl} plots of Ni_3Sn_4. (c) CV curve of 20 % Pt/C in 0.5 M H_2SO_4. (d) CV curves normalized by ECSA of Ni_3Sn_4 and 20 % Pt/C in 0.5 M H_2SO_4+ 1 M CH_3OH for MOR.*

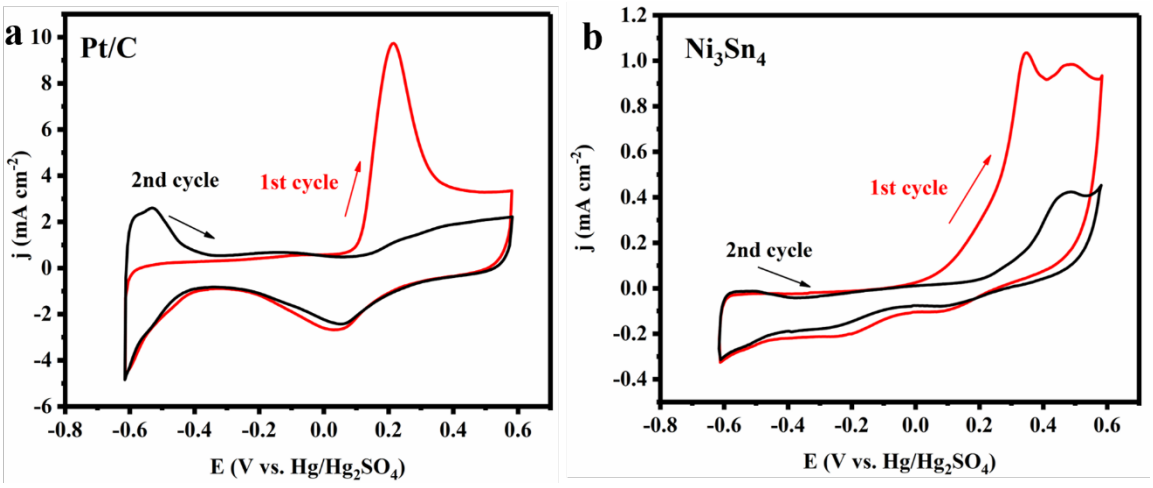

Figure S3. *CO stripping curves of (a) 20% Pt/C sample and (b) Ni_3Sn_4 sample in 0.5 M H_2SO_4 at the sweep rate of 50 mV/s.*

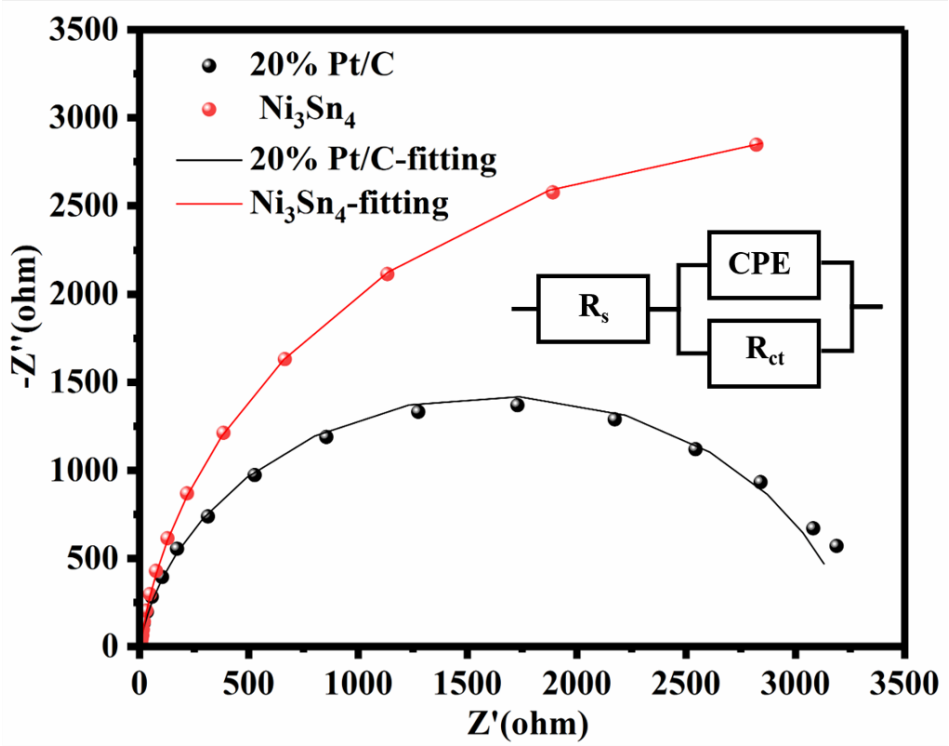

Figure S4. *Nyquist plots of Ni_3Sn_4 and 20% Pt/C in 0.5 M H_2SO_4 + 1 M CH_3OH at 0 V vs. Hg/Hg_2SO_4, and the inset is the equivalent circuit model diagram.*

Table S1. *The comparisons of MOR activity of Ni_3Sn_4 with some recently reported Pt-based catalysts.*

Catalysts	Electrolyte solution	scanning rate ($mV\ s^{-1}$)	Peak potential (V vs. RHE)	Reference

Ni_3Sn_4	0.5 M H_2SO_4+1 M CH_3OH	50	0.826	This work
PtCo CNCs	0.5 M H_2SO_4+1 M CH_3OH	50	0.881	[1]
Ce-modified Pt NPs	0.5 M H_2SO_4+1 M CH_3OH	50	0.851	[2]
$Pt/Ti_{0.95}Co_{0.05}N$	0.5 M H_2SO_4+1 M CH_3OH	50	0.857	[3]
Pt/TiN	0.5 M H_2SO_4+1 M CH_3OH	50	0.870	[4]
PtCo NCs	0.5 M H_2SO_4+0.5 M CH_3OH	50	0.863	[5]

S3. Theory: The atomic structure and energetics of oxidation and methanol oxidation were modeled by DFT-based methods implemented in the QUANTUM-ESPRESSO pseudopotential code [6] with the GGA–PBE + van der Waals (vdW) approximation [7]. This computational framework is feasible for the description of the interactions between molecules and similar surfaces surfaces. [8] The energy cutoffs were 25 and 400 Ry for the plane-wave expansion of the wave functions and the charge density, respectively. The 3×6×3 Monkhorst-Pack *k*-point grid for the Brillouin sampling was adopted for all considered systems. [9]

The values of the enthalpies of physical adsorption of the oxygen were calculated by following formula:

$\Delta H_{phys} = [E_{Ni3Sn4+O2} - (E_{Ni3Sn4} + E_{O2})]$, where E_{Ni3Sn4} is the total energy of pristine (010) surface of Ni_3Sn_4 and E_{O2} is the total energy of the single oxygen molecule in empty box. The energy of chemical adsorption is defined as the difference between the total energy of the system with physically adsorbed oxygen molecule and the total energy of the same system after decomposition of the oxygen molecule on the surface. The energies corresponding with the steps of methanol oxidation also defined as the difference between total energies of the system at these steps. Based on the methods reported in Ref. [10], we can use the values calculated for standard hydrogen electrode (SHE) as almost the same as the energies for reverse hydrogen electrode (RHE) in acidic media.

For the case of physical adsorption, we also estimated differential Gibbs free energy by following formula: $\Delta G = \Delta H - T\Delta S$, where T is the temperature and ΔS is the change of entropy of adsorbed molecule, which was estimated considering the gas→liquid transition by the standard formula: $\Delta S = \Delta H_{vaporization}/T$, where $\Delta H_{vaporization}$ is measured enthalpy of vaporization.

S4. X-ray absorption spectroscopy (XAS)

In order to obtain further insights into the oxidation status of Ni in our catalysts, we performed Xray absorption spectroscopy (XAS) measurements. Specifically, we probed the L3 absorption edge at 853 eV, which is associated with dipole-allowed 2p3/2→ 3d electronic transitions. This edge is particularly sensitive to local chemical modifications occurring in the immediate surroundings of the absorbing atoms, as d orbitals in Ni are involved in covalent bonds. Our results show that the L_3 absorption edges closely resemble the spectrum of metallic Ni, as evidenced by reference spectra for various oxidation states of Ni shown in the same Figure.

We note that XAS is not a routine characterization technique, as it requires the use of synchrotron radiation. Nevertheless, we consider it a valuable tool for the investigation of the electronic and chemical properties of our catalysts. In particular, the high sensitivity of XAS to local chemical environments makes it well-suited for probing the oxidation status of Ni in our system.

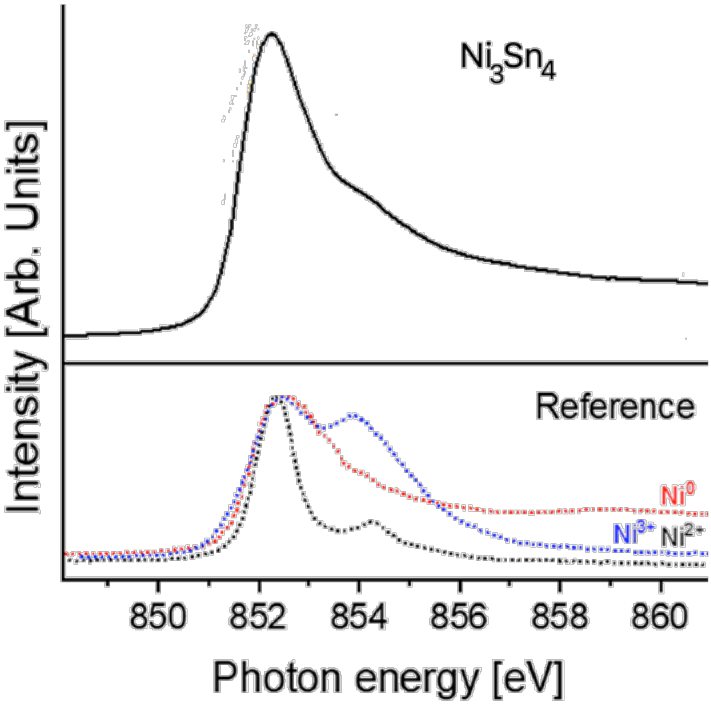

Figure S5: *L_3 absorption edge of Ni_3Sn_4 and reference spectra for the various oxidation states of Ni. The resemblance with the case of pure Ni is evident.*

S5. Further XPS data

XPS is a critical tool for characterizing the surface chemistry of materials. We would like to point out that in our study, XPS analysis was conducted using synchrotron radiation, which provides an extreme level of control over the measurement conditions. This enabled us to obtain highly precise core-level shifts for Ni and Sn, which are crucial for determining the oxidation state and electronic structure of the surface species. Additionally, we did perform a survey spectrum to assess the overall elemental composition of the samples. Survey spectra were repeated after having exposed the sample to an O_2 environment to probe surface oxidation and to air. We have revised the manuscript to include more details on the XPS analysis (Figure R10), including the specific region of interest and the measurement conditions. We hope these additions will better address the referee's concerns.

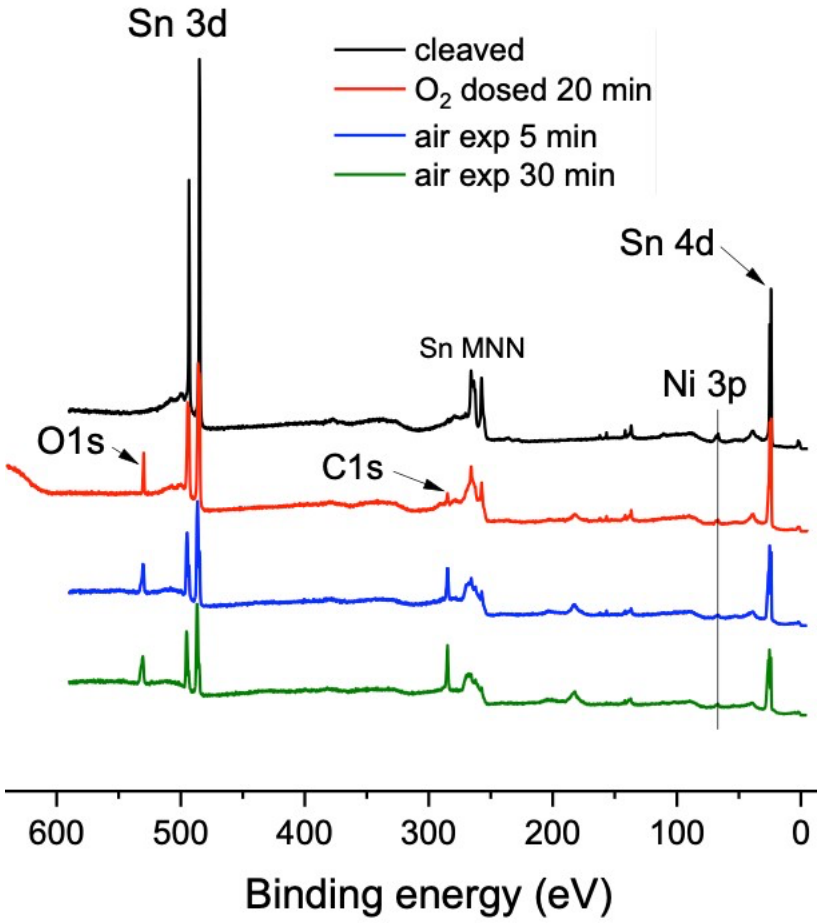

Figure S6: *Survey spectra for as-cleaved, O_2-dosed, air-exposed Ni_3Sn_4 surfaces.*

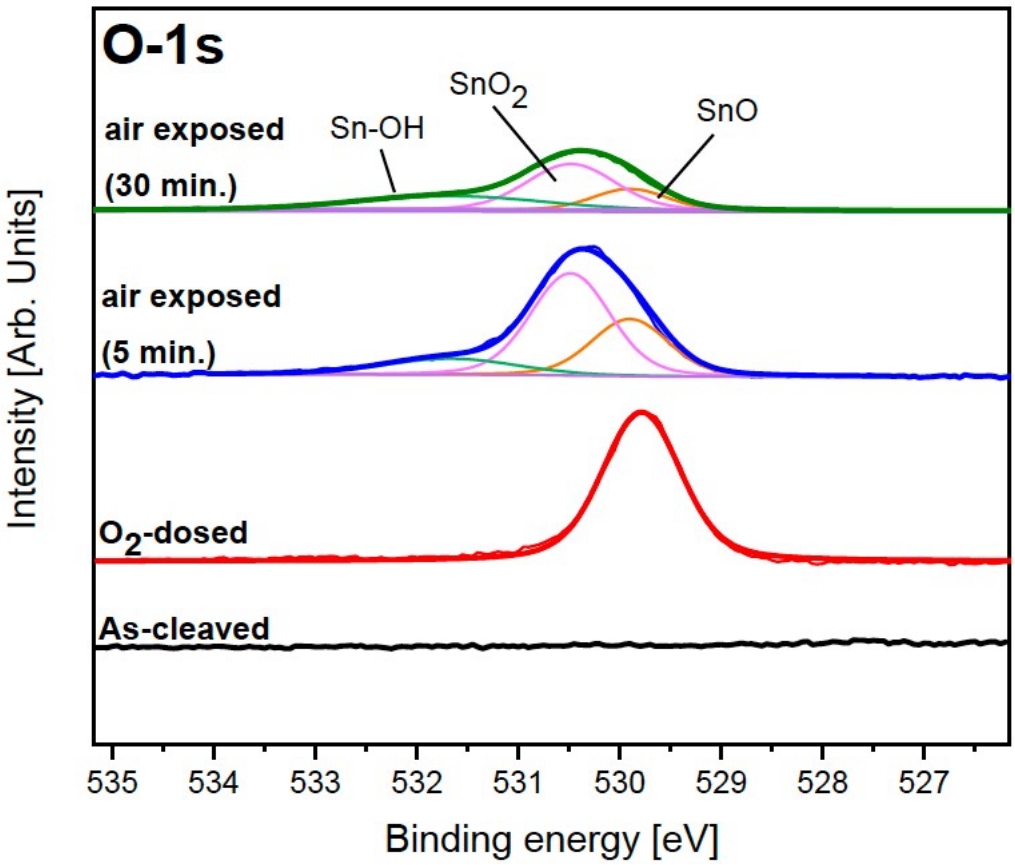

Figure S7*: O 1s core levels for as-cleaved Ni_3Sn_4 and after exposure to O_2 (20 minutes, $1x10^{-4}$ mbar), and air for 5 and 30 min. The photon energy is 590 eV.*

References

*[1] Z. Li, X. Jiang, X. Wang, J. Hu, Y. Liu, G. Fu and Y. Tang, Appl. Catal. B Environ., 2020, **277**, 119135.*

*[2] L. Chen, X. Liang, X. Li, J. Pei, H. Lin, D. Jia, W. Chen, D. Wang and Y. Li, Nano Energy, 2020, **73**, 104784.*

*[3] X. Chen, W. Li, Z. Pan, Y. Xu, G. Liu, G. Hu, S. Wu, J. Li, C. Chen and Y. Lin, Appl. Surf. Sci., 2018, **440**, 193-201.*

*[4] M. Yang, Z. Cuiw and F. J. DiSalvo, Phys. Chem. Chem. Phys., 2013, **15**, 1088-1092.*

*[5] Q. Chen, Z. Cao, G. Du, Q. Kuang, J. Huang, Z. Xie and L. Zheng, Nano Energy, 2017, **39**, 582589.*

[6] P. Giannozzi, S. Baroni, N. Bonini, M. Calandra, R. Car, C. Cavazzoni, D. Ceresoli, G. L. Chiarotti, M. Cococcioni, I. Dabo, A. Dal Corso, S. de Gironcoli, S. Fabris, G. Fratesi, R.

Gebauer, U. Gerstmann, C. Gougoussis, A. Kokalj, L. Michele, L. Martin-Samos, N. Marzari, F. Mauri, R.

*Mazzarello, S. Paolini, A. Pasquarello, L. Paulatto, C. Sbraccia, S. Scandolo, G. Sclauzero, A. P. Seitsonen, A. Smogunov, P. Umari, R. M. Wentzcovitch, J. Phys.: Cond. Matt. 2009, **21**, 395502. [7] J. P. Perdew, K. Burke, M. Ernzerhof, Phys. Rev. Lett. 1996, 77, 3865; b) V. Barone, M. Casarin, D. Forrer, M. Pavone, M. Sambi, A. Vittadini, J. Comput. Chem. 2009, **30**, 934.*

[8] NbAs https://doi.org/10.1002/adfm.201800511

*[9] H. J. Monkhorst, J. D. Pack, Phys. Rev. B 1976, **13**, 5188.*

[10] https://doi.org/10.1021/acs.jpcc.2c02734